

# The optical polarization of radio-loud and radio-intermediate broad absorption line quasi-stellar objects<sup>\*</sup>

D. Hutsemékers<sup>1,2,\*\*</sup> and H. Lamy<sup>2</sup>

<sup>1</sup> European Southern Observatory, Casilla 19001, Santiago 19, Chile

<sup>2</sup> Institut d'Astrophysique, Université de Liège, 5 av. de Cointe, 4000 Liège, Belgium

Received 6 January 2000 / Accepted 14 April 2000

**Abstract.** On the basis of a sample of approximately 50 broad absorption line quasi-stellar objects (BAL QSOs), we investigate possible correlations between BAL QSO radio properties and other spectral characteristics, including polarization. For this purpose new polarization data have been obtained.

The main result of our statistical study is the absence of significant correlations between the radio-to-optical flux ratio  $R^*$  and all other quantities: the polarization  $p_0$  of the continuum, the slope of the continuum, the balnicity and detachment indices which characterize the BAL profiles, and the terminal velocity of the flow  $v_{\max}$ . The claimed anticorrelation between  $R^*$  and  $v_{\max}$  is therefore not confirmed, as well as the correlation between  $R^*$  and  $p_0$  predicted by some models. Although marginally significant, the only possible correlations occur for the BAL QSOs with low-ionization troughs.

**Key words:** galaxies: quasars: absorption lines – galaxies: quasars: general – polarization

## 1. Introduction

About 12% of optically-selected QSOs exhibit broad absorption lines (BALs) in their spectrum, that is resonance line absorption troughs that extend blueward of the emission lines up to  $\sim 0.1 c$ . Since the continuum and emission line properties of most BAL QSOs are not found to significantly differ from those of normal (non-BAL) QSOs, it is generally thought that rapidly moving absorbing matter exists in all (at least all radio-quiet) QSOs with a small covering factor, the BAL QSOs being those objects with the absorption region (the BALR) along the line of sight (Junkkarinen 1983, Weymann et al. 1991). Alternatively, if one focuses on the different behavior of the rarer objects with low-ionization absorption troughs, BAL QSOs could constitute a distinct population of QSO, possibly in a different evolutionary stage (Boroson & Meyers 1992). An important characteristic

of BAL QSOs is the absence of powerful radio-sources among them (Stocke et al. 1992, Kuncic 1999).

The hypothesis that all radio-quiet QSOs are surrounded by a BALR implies that all differences between BAL and non-BAL QSOs are due to orientation. There are at least two important differences between BAL and non-BAL QSOs: as a class, BAL QSOs are more polarized than non-BAL QSOs (Stockman et al. 1984, Hutsemékers et al. 1998, Schmidt & Hines 1999), and they are more frequently found among radio-intermediate QSOs (Francis et al. 1993). To interpret these differences within the orientation –or unification– model, Goodrich (1997) has suggested that at least some BAL QSOs must have an attenuated direct continuum along our line of sight, such that the scattered light is more important in the total light we see, and then the observed polarization is larger than in non-BAL QSOs. Such an attenuation simultaneously explains why some BAL QSOs dominate the radio-intermediate class: the optical continuum is fainter, and the ratio of radio to optical fluxes is higher. This also means that the true fraction of BAL QSOs in optically-selected samples could be severely underestimated (Goodrich 1997).

The main goal of the present paper is to verify a direct consequence of this interpretation: the existence of a correlation between the optical continuum polarization of BAL QSOs and their radio-to-optical flux ratio. We have therefore compiled linear polarization measurements for a sample of BAL QSOs with known radio properties, essentially taken from the Stocke et al. (1992) VLA radio survey. Additional polarization data have been obtained for BAL QSOs with more extreme radio properties, including the five radio-loud BAL QSOs recently discovered by Brotherton et al. (1998). Furthermore, we investigate possible correlations between absorption line indices and radio properties, and more particularly the claimed anticorrelation between the terminal velocity of the flow and the radio-to-optical flux ratio (Weymann 1997). This relation, if confirmed, provides strong constraints on theoretical models, and may constitute a clue to the radio-loud / radio-quiet dichotomy in QSOs (Murray et al. 1995, Kuncic 1999).

The paper is organized as follows: in Sect. 2, we present the data, new measurements and compilation. The statistical analysis and the results are presented in Sect. 3. Discussion and conclusions form the last section.

<sup>\*</sup> Based on observations collected at the European Southern Observatory (ESO, La Silla)

<sup>\*\*</sup> Also, Chercheur Qualifié au Fonds National de la Recherche Scientifique (FNRS, Belgium)

**Table 1.** The sample of BAL QSOs with measured radio flux and polarization

Object	$z$	Type	BI	$v_{\max}$	DI	$\alpha_B$	$p_0$	$\log R^*$	$\log L_{\text{rad}}$	Ref
B0004+0147	1.71	4	255	>25000	-	-	1.26	< 0.04	< 24.50	3
B0019+0107	2.12	2	2305	13383	4.65	0.73	0.85	< -0.14	< 24.59	1
B0021-0213	2.30	2	5180	12545	3.14	0.66	0.63	< 0.10	< 24.69	1
B0025-0151	2.07	2	2878	22415	2.97	0.34	0.37	< -0.01	< 24.70	1
B0029+0017	2.23	2	5263	10738	2.45	0.55	0.68	< 0.05	< 24.62	1
B0043+0048	2.14	5	4452	17705	10.06	-0.13	0.00	0.76	25.78	1
B0059-2735	1.59	3	11054	18544	1.18	1.50	1.60	< 0.09	< 24.49	1
B0137-0153	2.23	2	4166	9126	2.41	1.01	1.08	0.65	25.26	1
B0145+0416	2.03	2	4765	14480	3.96	0.96	2.68	< -0.50	< 24.38	1
B0146+0142	2.89	-	5523	20866	4.87	0.79	1.21	< -0.56	< 24.87	3
B0226-1024	2.26	2	7373	21834	4.72	0.88	2.50	< -0.38	< 24.76	3
B0254-3327	1.86	2	694	4223	1.08	0.64	0.00	< 0.54	< 24.73	1
B0846+1540	2.91	-	-	-	-	-	0.77	< -0.26	< 24.78	2
B0856+1714	2.32	-	8590	16802	5.43	-	0.66	1.05	25.65	2
B0903+1734	2.78	-	9776	16480	4.34	1.54	0.88	< -0.35	< 24.84	1
B0932+5006	1.91	4	6636	18157	3.88	0.93	1.38	< -0.39	< 24.55	3
B0946+3009	1.22	2	-	-	-	-	0.84	: -1.75	: 23.20	3
B1009+0222	1.35	2	1565	12029	2.02	-	0.75	0.49	24.49	2
B1011+0906	2.26	3	5587	>25000	6.84	1.95	2.10	< -0.38	< 24.67	1
B1029-0125	2.04	2	1849	18738	2.22	0.83	1.09	< 0.11	< 24.56	1
J 1053-0058	1.55	3	255	5300	1.20	0.74	1.89	1.98	25.84	2
J 1104-0004	1.35	3	-	-	-	-	0.45	2.49	25.90	2
B1120+0154	1.47	5	415	9884	0.79	0.45	1.93	< -0.50	< 24.16	1
J 1141-0141	1.27	3	-	-	-	-	0.32	1.73	24.98	2
B1212+1445	1.62	5	3619	19189	6.05	1.51	1.42	0.11	24.62	1
B1216+1103	1.62	2	4792	11900	4.66	0.18	0.55	< 0.24	< 24.50	2
J 1225-0150	2.04	2	3900	24300	7.20	1.50	0.77	1.38	25.19	2
B1228+1216	1.41	2	496	21512	7.17	-	0.00	< -0.38	< 24.17	2
B1230+1705	1.42	2	-	-	-	-	0.25	: -0.09	: 24.23	2
B1231+1320	2.39	4	3473	>25000	6.38	2.15	0.68	< -0.01	< 24.62	1
B1232+1325	2.36	3	12620	>25000	1.84	2.38	1.99	< 0.08	< 24.67	1
B1235+0857	2.89	-	815	4997	0.42	1.04	2.27	0.08	25.09	1
B1235+1807	0.45	3	-	-	-	-	0.00	0.71	24.22	2
B1246-0542	2.22	5	4309	22995	6.60	1.84	0.87	0.06	25.14	1
J 1252+0053	1.69	2	130	15400	5.20	0.64	0.14	2.01	25.73	2
B1254+0443	1.02	2	-	-	-	-	0.58	-0.84	24.01	3
B1309-0536	2.21	2	5363	>25000	5.10	1.41	0.73	< -0.77	< 24.25	1
B1331-0108	1.87	3	7912	21963	1.15	2.66	1.86	0.61	25.24	1
B1333+2840	1.91	2	2357	9448	2.20	0.77	5.88	< -0.03	< 24.59	2
B1413+1143	2.54	5	6621	12351	1.50	1.72	1.50	0.29	25.55	1
B1429-0036	1.18	2	-	-	-	-	0.00	< -0.07	< 24.13	2
B1442-0011	2.22	2	5143	21963	2.83	0.58	0.00	: -0.19	: 24.52	1
B1443+0141	2.45	-	7967	24673	3.26	0.60	1.31	< -0.16	< 24.69	2
B1700+5153	0.29	3	-	-	-	-	0.58	0.56	24.39	3
B2225-0534	1.98	4	7903	15512	0.48	1.68	4.36	< 0.09	< 24.78	1
B2240-3702	1.84	5	8539	23253	0.69	1.08	2.08	< -0.30	< 24.47	1
B2241+0016	1.39	2	-	-	-	-	0.57	< 0.15	< 24.30	3
B2341-2333	2.82	-	-	-	-	-	0.61	0.19	25.23	2
B2350-0045	1.63	4	6964	22995	5.08	1.01	0.53	< 0.28	< 24.50	1

Units: BI and  $v_{\max}$  are in  $\text{km s}^{-1}$ ,  $p_0$  in%, and  $L_{\text{rad}}$  in  $\text{W Hz}^{-1}$ . Uncertain radio measurements are indicated (:)

Object Type: (2) HIBAL QSOs, (3) Strong LIBAL QSOs, (4) Weak LIBAL QSOs, (5) Marginal LIBAL QSOs

References for polarization: (1) Hutsemékers et al. 1998, (2) Lamy & Hutsemékers 2000, (3) Schmidt & Hines 1999

## 2. The data

The considered sample is constituted of BAL QSOs with measured radio flux and good quality broad-band polarization data

compiled from the literature. It also includes polarization measurements specifically obtained for the present study. This sample is given in Table 1. Table 2 contains additional BAL QSOs

for which only radio flux and absorption line indices are available.

Tables 1 and 2 list the QSO position-name (B1950 or J2000), the redshift  $z$ , and the object type / classification which depends on the presence of low-ionization BAL troughs. The balnicity index BI, the maximum velocity  $v_{\max}$ , and the detachment index DI are quantities which characterize the BALs, while  $\alpha_B$  is the continuum power-law index, and  $p_0$  the debiased polarization degree.  $R^*$  is the K-corrected radio-to-optical flux ratio, and  $L_{\text{rad}}$  the radio power at 5 GHz. Details on these quantities are given below.

### 2.1. The radio data

Most radio measurements are from the Stocke et al. (1992) BAL QSO VLA radio survey at 5 GHz. This sample provides a homogeneous set of K-corrected radio-to-optical flux ratios, and of radio powers in  $\text{W Hz}^{-1}$ , K-corrected to 5 GHz in the QSO rest-frame.

For only one object of our previous polarization survey (Hutsemékers et al. 1998, hereafter Paper I), B1120+0154 (= UM425), an additional radio measurement is found in the literature (Meylan & Djorgovski 1989). It is included in Table 1 after computing  $R^*$  and  $L_{\text{rad}}$  following the prescriptions of Stocke et al. (1992).

Since then, a handful of radio-loud BAL QSOs has been discovered by Brotherton et al. (1998). These five unusual objects (with J2000 coordinates) are also included in our sample. The K-corrected radio-to-optical flux ratios are from Brotherton et al. (1998), while the radio powers have been computed and K-corrected to 5 GHz according to Stocke et al. (1992). None of these formally radio-loud<sup>1</sup> BAL QSOs appear to be powerful radio sources (i.e. all have  $\log R^* \lesssim 2.5$ ; see also the discussion by Kuncic 1999).

### 2.2. The polarization

Most polarization data come from our previous survey (Paper I). However this sample was not chosen to investigate possible correlations with radio properties, and additional measurements were needed. Using the ESO 3.6m telescope + EFOOSC, we then obtained new broad-band linear polarization data for 16 BAL QSOs, most of them with extreme radio properties, i.e. with the highest  $R^*$  values or with stringent upper limits. These data are presented in Lamy & Hutsemékers (2000) with full account of the observation and reduction details. We also refer the reader to Paper I and to Lamy & Hutsemékers (1999) for details related to our previous survey and to reduction procedures. The polarization degree  $p_0$  reported in Table 1 is debiased according to the Wardle & Kronberg (1974) method. Typical uncertainties of the polarization degree are 0.2–0.3%.

<sup>1</sup> QSOs with  $\log R^* \geq 1$  are considered as formally radio-loud. As a definition of radio-intermediate QSOs, we adopt  $0 < \log R^* < 1$ , in order to encompass objects classified as such by Francis et al. (1993). Radio-quiet QSOs have  $\log R^* \leq 0$

Independently of our survey, Schmidt & Hines (1999) have recently published a large number of BAL QSO polarization data, obtained mostly in white light. For the sake of homogeneity, we consider in Table 1 only the BAL QSOs of their sample with polarization degrees sufficiently accurate, i.e. with  $\sigma_p \leq 0.4\%$ ,  $\sigma_p$  denoting the uncertainty of the observed polarization degree  $p$ . This constraint, also applied to our data, is important since several BAL QSOs have low polarization levels ( $p \leq 1\%$ ). 8 BAL QSOs from the Schmidt & Hines (1999) sample and with available radio measurements are then added to our sample. Their polarization degrees have been similarly debiased. The data of Schmidt & Hines (1999) also confirm our previous measurement of the polarization of B0145+0416, which was questioned in Paper I. Note finally that their spectropolarimetric data clearly show that broad-band polarization measurements represent fairly well the polarization of the continuum.

### 2.3. The spectral indices

Weymann et al. (1991) provide a series of useful spectral indices to characterize the absorption features of BAL QSOs. They define the balnicity index BI which is a modified velocity equivalent width of the C IV  $\lambda 1549$  BAL, and the detachment index DI which measures the onset velocity of the strongest C IV BAL trough in units of the adjacent emission line half-width, that is the degree of detachment of the absorption line relative to the emission one (cf. Weymann et al. 1991 for more details). C IV BI and DI are reported in Tables 1 and 2. When BI are also given by Korista et al. (1993), we adopt an average of these values and those of Weymann et al. (1991). For the radio-loud BAL QSOs, BI are from Brotherton et al. (1998). We do not consider BI measured from other BAL troughs.

For a few BAL QSOs of our sample, the C IV DI are not given by Weymann et al. (1991). Therefore, as in Paper I, we have computed them by using good quality published spectra, when available. The spectra were digitally scanned, and the measurements done following the prescriptions by Weymann et al. (1991). The new measurements make use of spectra published by Korista et al. (1993) and Brotherton et al. (1998), and are reported in Tables 1 and 2 together with values from Paper I. Only one object (B0004+0147) with a spectrum in Korista et al. (1993) has no measured DI, due to an unusual emission line profile.

In addition to BI and DI, we have also reported in Tables 1 and 2 the maximum velocity in the C IV BAL trough,  $v_{\max}$ , which provides an estimate of the terminal velocity of the flow. For the radio-loud BAL QSOs, values of  $v_{\max}$  are given by Brotherton et al. (1998). For other objects,  $v_{\max}$  is evaluated from the Korista et al. (1993) and Steidel & Sargent (1992) spectra, by measuring, from the blue to the red, the wavelength at which the absorption first drops  $\sim 10\%$  below the flux level defined by the local continuum (cf. also Lee & Turnshek 1995). Narrow or weak high-velocity absorption features are not taken into account. Further, at velocities higher than  $\sim 25000 \text{ km s}^{-1}$ , C IV BALs may be contaminated by the Si IV emission line, such

**Table 2.** Additional BAL QSOs with measured radio flux and BAL indices

Object	$z$	Type	BI	$v_{\max}$	DI	$\alpha_B$	$\log R^*$	$\log L_{\text{rad}}$
B0135–4001	1.85	-	3577	17834	7.38	-	$< -0.46$	$< 24.53$
B0324–4047	3.06	-	3614	19899	5.00	-	$< -0.19$	$< 25.21$
B1208+1535	1.96	2	4545	17770	4.64	0.42	$< -0.03$	$< 24.60$
B1235+1453	2.68	-	2658	13835	3.55	1.01	$< 0.13$	$< 24.92$
B1240+1607	2.36	2	2867	21382	4.47	1.06	$< 0.09$	$< 24.71$
B1243+0121	2.79	-	5953	15319	2.35	1.17	$< -0.03$	$< 24.84$
B1303+3048	1.76	2	1897	10996	2.27	0.57	$< -0.42$	$< 24.60$
B1314+0116	2.69	-	2626	13899	7.41	0.64	$< -0.03$	$< 24.77$
B1336+1335	2.43	-	5973	15448	1.18	-	$< 0.52$	$< 24.85$
B1414+0859	2.64	-	3516	$>25000$	11.00	-	$< 0.49$	$< 24.70$
B1504+1041	3.07	-	4140	17834	3.23	-	$< 0.71$	$< 24.91$
B2201–1834	1.82	5	1613	19963	2.19	2.37	$< -0.34$	$< 24.55$
B2212–1759	2.21	-	2221	8480	6.70	-	$< -0.14$	$< 24.70$

Units and Object Type are as in Table 1

that the measurement of  $v_{\max}$  becomes inaccurate. We therefore limit  $v_{\max}$  to  $25000 \text{ km s}^{-1}$  from the C IV emission centroid, in agreement with the definition of BI (Weymann et al. 1991). This limit constitutes, in a few cases, a lower limit to the true  $v_{\max}$ .

Finally, we have measured the slope of the continuum as in Paper I. Using spectra published by Weymann et al. (1991) and by Brotherton et al. (1998), a power-law continuum  $F_\nu \propto \nu^{-\alpha}$  was fitted blueward of C III]  $\lambda 1909$  (cf. Paper I). The resulting index  $\alpha_B$  is provided in Tables 1 and 2.

#### 2.4. The LIBAL / HIBAL classification

Approximately 15% of BAL QSOs have deep low-ionization BALs (Mg II  $\lambda 2800$  and/or Al III  $\lambda 1860$ ) in addition to the usual high-ionization troughs (Weymann et al. 1991, Voit et al. 1993). These objects could be significantly reddened by dust (Sprayberry & Foltz 1992). Since they have no or very weak [O III]  $\lambda 5007$  emission compared to other objects, Boroson & Meyers (1992) have argued that LIBAL QSOs are not seen along a preferred line of sight but could constitute a physically different class of BAL QSOs.

In Paper I, we have defined three categories of LIBAL QSOs: strong (S), weak (W), and marginal (M) LIBAL QSOs. Indeed, in addition to the strong and weak LIBAL QSOs, first classified as such by Weymann et al. (1991), several authors have reported faint LIBAL features in a number of other objects (Hartig & Baldwin 1986, Hazard et al. 1984). We have classified the latter objects as marginal LIBAL QSOs. They are characterized by very weak Mg II and/or Al III BALs. The asymmetry of the Mg II or C III] emission lines, when cut on the blue side, is also considered as evidence for marginal LIBALs (Hartig & Baldwin 1986). BAL QSOs with no evidence for low-ionization features are classified as high-ionization (HI) BAL QSOs. Objects with poor quality spectra, or objects with no Al III BAL and Mg II outside the observed spectral range, remain unclassified (cf. Paper I for additional details and examples). It is important to note that the present classification somewhat differs from other classifications found in the literature. Most often, the BAL QSOs defined

in the literature as low-ionization BAL QSOs are the S-LIBALs or the S-LIBALs + W-LIBALs, while the high-ionization BAL QSOs are anything else, including M-LIBALs and unclassified objects.

Our classification is summarized in Tables 1 and 2. It is based on a careful inspection of good-quality spectra available in the literature (Brotherton et al. 1998, Foltz et al. 1987, 1989, Hewett et al. 1991, Steidel & Sargent 1992, Turnshek et al. 1985, Turnshek & Grillmair 1986, Turnshek 1988, Wampler 1983, Weymann et al. 1991). Several BAL QSO sub-types were already given and discussed in Paper I.

### 3. Results of statistical tests

Before presenting the results of the statistical tests, it is immediately clear from Table 1 that radio-intermediate and radio-loud BAL QSOs are not the most polarized objects. Among the five radio-loud BAL QSOs from Brotherton et al. (1998), only one, J1053-0058, which belongs to the LIBAL class, is significantly polarized with  $p_0 \simeq 1.9\%$ . It is particularly interesting to note that J1053-0058 has the smallest detachment index among the radio-loud BAL QSOs, in good agreement with the anticorrelation between  $p_0$  and DI found in Paper I<sup>2</sup>.

Since  $R^*$  and  $L_{\text{rad}}$  are often upper limits, the search for possible correlations between  $\log R^*$  (or  $\log L_{\text{rad}}$ ) and other BAL QSO properties must rely on survival analysis. We then use the standard survival analysis tests available in the ASURV Rev. 1.3 package (LaValley et al. 1992). Several sub-samples are considered: LIBAL QSOs, HIBAL QSOs, and BAL QSOs with  $z > 1.5$ . The latter limit corresponds to the redshift at which the C IV BAL starts to be detected in the visible. Probabilities ( $P$ ) that the observed statistics occur by chance among indices uncorrelated with  $\log R^*$  are summarized in Table 3, using the generalized Kendall  $\tau$  and Spearman  $\rho$  rank order correlation coefficients, and the Cox proportional hazard model (LaValley

<sup>2</sup> The anticorrelation between  $p_0$  and DI is confirmed and even more significant when taking into account the polarization data presented here (i.e. with 37 BAL QSOs instead of 29 in Paper I)

**Table 3.** Analysis of correlation of various indices with  $\log R^*$ 

	$p_0$	BI	DI	$\alpha_B$	$-v_{\max}$	
All BALs	0.09	0.45	0.93	0.61	-	C
	0.11	0.44	0.92	0.58	0.20	K
	0.05	0.45	0.72	0.91	0.15	S
	—	—	—	+	+	
	49/28	51/38	50/37	41/30	51/38	n/m
HI BALs	0.29	0.44	0.85	0.35	-	C
	0.97	0.16	0.71	0.22	0.93	K
	0.49	0.24	0.72	0.83	0.62	S
	—	—	—	+	+	
	22/14	20/15	20/15	18/14	20/15	n/m
LI BALs	<b>0.03</b>	0.56	0.38	0.50	-	C
	<b>0.03</b>	0.58	0.74	0.51	<b>0.04</b>	K
	<b>0.03</b>	0.95	0.70	0.65	0.06	S
	—	+	+	-	+	
	20/10	17/11	16/10	16/10	17/11	n/m
All BALs	0.19	0.38	0.75	0.70	-	C
$z > 1.5$	0.32	0.49	0.71	0.67	0.24	K
	0.11	0.30	0.85	0.89	0.15	S
	—	—	—	—	+	
	37/24	48/36	47/35	40/29	48/36	n/m

This table gives the probabilities that the observed statistics (Cox, Kendall, Spearman) occur by chance among uncorrelated quantities.  $n$  is the number of objects considered in the correlation analysis, and  $m$  the number of objects with  $\log R^*$  upper limits. The sign of the correlation is also given, from the sign of the Spearman  $\rho$ . The three less accurate values of  $\log R^*$  are considered as detections, although the results are unchanged if they are not taken into account. The Cox model cannot be used to test correlations with  $-v_{\max}$ , since  $-v_{\max}$  is also left-censored. Some results, obtained with very few detections and given here for completeness, must be seen with caution

et al. 1992, Isobe et al. 1986). Results from Table 3 indicate that  $\log R^*$  is essentially uncorrelated with the other quantities ( $P \geq 0.05$ ), except within the LIBAL QSO sub-sample. The statistical analysis includes the few radio-loud BAL QSOs. Indeed, these objects, although formally radio-loud, are not powerful radio-sources and mostly in the radio-quiet / radio-loud transition region. However, since the original suggestion by Goodrich (1997) only includes formally radio-intermediate objects, we have also considered the sample of BAL QSOs with  $\log R^* < 1$ . In this case, the results of Table 3 are basically unchanged,  $P$  being only slightly higher for the weak correlations detected in the LIBAL QSO sub-sample. Finally the same statistical analysis has been carried out considering  $\log L_{\text{rad}}$  instead of  $\log R^*$ , with the result that  $\log L_{\text{rad}}$  is totally uncorrelated with the other quantities, whatever the sub-sample.

Within the LIBAL QSO sub-sample, the statistical tests suggest the existence of a weakly significant anticorrelation between  $\log R^*$  and  $p_0$  ( $P \leq 0.05$  for all tests), and a marginally significant anticorrelation between  $\log R^*$  and  $v_{\max}$  ( $P \leq 0.05$  for only one test). We have therefore plotted  $p_0$  and  $v_{\max}$  against  $\log R^*$  in Figs. 1 and 2. The anticorrelations do not appear very convincing. And indeed, if we delete only one object from the

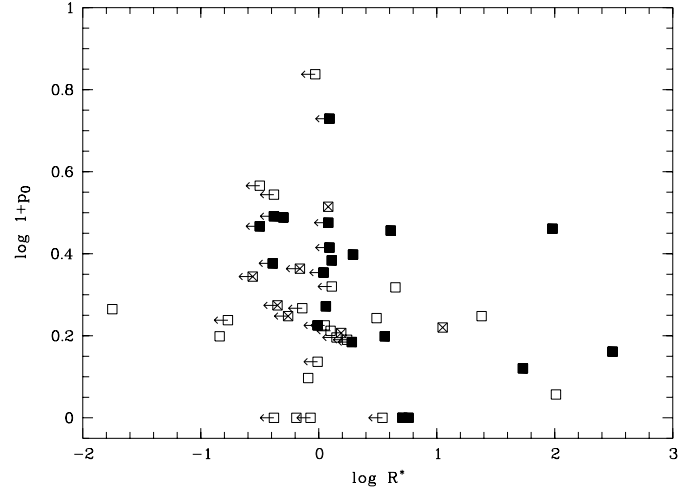


**Fig. 1.** The BAL QSO polarization,  $p_0$ , is plotted here against the radio-to-optical flux ratio,  $R^*$ . Censored data points are indicated. Open squares represent HIBAL QSOs, filled squares LIBAL QSOs, and squares with a cross unclassified BAL QSOs

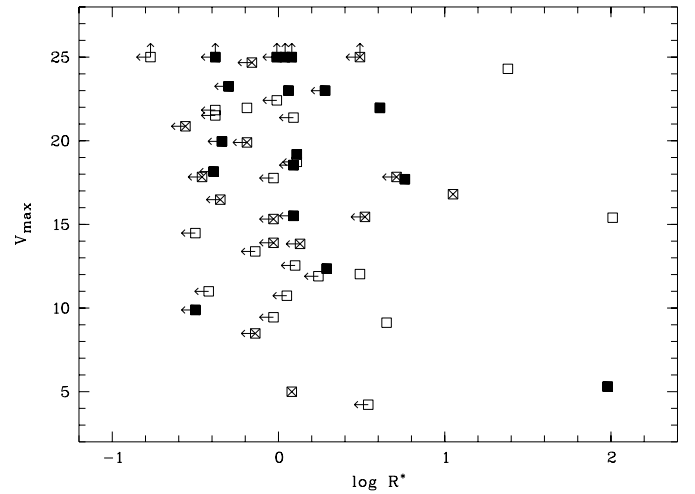


**Fig. 2.** The CIV BAL maximum velocity,  $v_{\max}$ , is plotted here against the radio-to-optical flux ratio,  $R^*$ . Censored data points are indicated. Open squares represent HIBAL QSOs, filled squares LIBAL QSOs, and squares with a cross unclassified BAL QSOs

LIBAL QSO sub-sample (e.g. B2225-0534 in Fig. 1, and J1053-0058 in Fig. 2), the statistical tests indicate that the correlations are not significant any longer. Further, if one restricts the LIBAL QSO sub-sample to high-redshift objects ( $z > 1.5$ ), the correlation between  $p_0$  and  $\log R^*$  disappears ( $P > 0.35$  with  $n/m = 15/9$ ), suggesting a possible bias. Note that due to the limited sample of LIBAL QSOs, no distinction between LIBAL sub-types was made.

In view of the apparently different behavior of LIBAL QSOs, we have also compared the distribution of  $\log R^*$  for the LIBAL and HIBAL QSO sub-samples, again using standard survival analysis tests from the ASURV package. Tests include the Logrank test, and the Gehan, Peto & Peto, and Peto & Prentice generalized Wilcoxon tests (LaValley et al. 1992,

Feigelson et al. 1985). The probability that the two samples (25 HIBALs and 21 LIBALs) are drawn from the same parent population is found to range from 0.06 to 0.09, depending on the test. This means that no significant difference in the distribution of  $\log R^*$  is detected when comparing the LIBAL and HIBAL QSO sub-samples.

#### 4. Discussion and conclusions

On the basis of a sample of approximately 50 BAL QSOs, we have investigated possible correlations between BAL QSO radio properties and other spectral characteristics, including polarization and the terminal velocity of the flow.

The main result of our statistical study is the absence of correlations between the radio-to-optical flux ratio,  $R^*$ , and all other quantities: polarization and slope of the continuum, balnicity and detachment indices, and the terminal velocity of the flow. The anticorrelation between  $R^*$  and  $v_{\max}$  claimed by Weymann (1997) and Kuncic (1999) is therefore not confirmed. Furthermore, we do not support the relation between  $R^*$  and  $p_0$  suggested by the model of Goodrich (1997), even if we restrict our sample to the formally radio-intermediate objects.

The only possible correlations occur within the LIBAL QSO sub-sample, which, once more, seems to behave differently. But the significance is marginal and additional data are necessary. It is nevertheless important to remark that, if real, the relation between  $R^*$  and  $p_0$  is opposite to the prediction of Goodrich (1997) who suggests that  $p_0$  would be higher for objects with large  $R^*$  as a result of a stronger attenuation of the UV rest-frame continuum.

It is also interesting to note that  $R^*$  is uncorrelated with the continuum power-law index  $\alpha_B$ , i.e. with dust extinction (Sprayberry & Foltz 1992). This is in agreement with the results of Hall et al. (1997) who found, from the distribution of optical / near-infrared colours, that the excess of BAL QSOs among radio-intermediate QSOs cannot be attributed to extinction.

Within the unification scheme, different orientation and attenuation of the continuum are probably necessary to explain the different polarization properties of BAL and non-BAL QSOs (Goodrich 1997). Our results indicate that this interpretation cannot simultaneously explain the excess of BAL QSOs among radio-intermediate QSOs. Another interpretation of BAL QSO radio properties is therefore needed.

Alternatively, we may abandon the hypothesis that all observed differences between BAL and non-BAL QSOs are only due to different orientations. The BAL phenomenon may then be seen as an evolutionary mass-loss phase, and properties like polarization could be related to the presence of ejected material. The range of BAL QSO radio properties can also be explained considering models like that of Kuncic (1999) which associates the BAL region with a poorly collimated and weakly radio-emitting jet. The lack of correlation between  $v_{\max}$  and  $R^*$  does

not support this model, although it should be pointed out that it does not necessarily refute it. Indeed, the relation between  $v_{\max}$  and  $R^*$  may depend on several other parameters, like the covering factor or the orientation of the jet. In this view, the eventual detection of a significant anticorrelation between  $v_{\max}$  and  $R^*$  within a larger LIBAL QSO sub-sample would fix some of these parameters, and provide useful constraints on the models.

*Acknowledgements.* The SIMBAD database operated by the CDS has been consulted. HL is supported in part by contracts ARC 94/99-178 and PAI P4/05. The referee is acknowledged for useful comments.

#### References

- Boroson T.A., Meyers K.A., 1992, ApJ 397, 442  
 Brotherton M.S., van Breugel W., Smith R.J., et al., 1998, ApJ 505, L7  
 Feigelson E.D., Nelson P.I., 1985, ApJ 293, 192  
 Foltz C.B., Chaffee F.H., Hewett P.C., et al. 1987, AJ 94, 1423  
 Foltz C.B., Chaffee F.H., Hewett P.C., et al. 1989, AJ 98, 1959  
 Francis P.J., Hooper E.J., Impey C.D., 1993, AJ 106, 417  
 Goodrich R.W., 1997, ApJ 474, 606  
 Hall P.B., Martini P., DePoy D.L., Gatley I., 1997, ApJ 484, L17  
 Hartig G.F., Baldwin J.A., 1986, ApJ 302, 64  
 Hazard C., Morton D.C., Terlevich R., McMahon R., 1984, ApJ 282, 33  
 Hewett P.C., Foltz C.B., Chaffee F.H., 1991, AJ 101, 1121  
 Hutsemékers D., Lamy H., Remy M., 1998, A&A 340, 371 (Paper I)  
 Isobe T., Feigelson E.D., Nelson P.I., 1986, ApJ 306, 490  
 Junkkarinen V.T., 1983, ApJ 265, 73  
 Korista K.T., Voit G.M., Morris S.L., Weymann R.J., 1993, ApJS 88, 357  
 Kuncic Z., 1999, PASP 111, 954  
 Lamy H., Hutsemékers D., 1999, The Messenger 96, 25 (Erratum: The Messenger 97, 23)  
 Lamy H., Hutsemékers D., 2000, A&AS 142, 451  
 LaValley M., Isobe T., Feigelson E.D., 1992, BAAS 24, 839  
 Lee L.W., Turnshek D.A., 1995, ApJ 453, L61  
 Meylan G., Djorgovski S., 1989, ApJ 338, L1  
 Murray N., Chiang J., Grossman S.A., Voit G.M., 1995, ApJ 451, 498  
 Schmidt G.D., Hines D.C., 1999, ApJ 512, 125  
 Sprayberry D., Foltz C.B., 1992, ApJ 390, 39  
 Steidel C.C., Sargent W.L.W., 1992, ApJS 80, 1  
 Stocke J.T., Morris S.L., Weymann R.J., Foltz C.B., 1992, ApJ 396, 487  
 Stockman H.S., Moore R.L., Angel J.R.P., 1984, ApJ 279, 485  
 Turnshek D.A., Foltz C.B., Weymann R.J., et al., 1985, ApJ 294, L1  
 Turnshek D.A., Grillmair C.J., 1986, ApJ 310, L1  
 Turnshek D.A. 1988, in: Blades J.C. et al. (eds), QSO absorption Lines: Probing the Universe, Cambridge, p. 17  
 Voit G.M., Weymann R.J., Korista K.T., 1993, ApJ 413, 95  
 Wampler E.J., 1983, A&A 122, 54  
 Wardle J.F.C., Kronberg P.P., 1974, ApJ 194, 249  
 Weymann R.J., Morris S.L., Foltz C.B., Hewett P.C., 1991, ApJ 373, 23  
 Weymann 1997, in: Arav N., et al. (eds), Mass Ejection from Active Galactic Nuclei, ASP Conference Series 128, p. 3